Talanta 122 (2014) 293–301

Contents lists available at ScienceDirect

Talanta

journal homepage: www.elsevier.com/locate/talanta

Direct quantitative analysis of aromatic amino acids in human plasma by four-way calibration using intrinsic fluorescence: Exploration of third-order advantages

Chao Kang, Hai-Long Wu*, Li-Xia Xie, Shou-Xia Xiang, Ru-Qin Yu

State Key Laboratory of Chemo/Biosensing and Chemometrics, College of Chemistry and Chemical Engineering, Hunan University, Changsha 410082, China

ARTICLE INFO

Article history:
Received 4 November 2013
Received in revised form
7 January 2014
Accepted 11 January 2014
Available online 31 January 2014

Keywords:
Four-way calibration
Quadrilinear component model
Third-order advantage
Fluorescence
Aromatic amino acids

ABSTRACT

A novel intrinsic fluorescence method for the direct determination of L-phenylalanine, L-tyrosine, and L-tryptophan in human plasma is presented. By using fluorescence excitation–emission–pH–sample data array in combination with four-way calibration method based on the quadrilinear component model, the proposed approach successfully achieved quantitative analysis of the aromatic amino acids in human plasma, even in the presence of an unknown, uncalibrated serious interferent. It needs little preparation, uses the "mathematical separation" instead of "analytical separation", what makes it fast and environmentally friendly. Satisfactory results have been achieved for calibration set, validation set, and prediction set. The ranges for phenylalanine, tyrosine, and tryptophan are 2.0×10^3–20.0×10^3, 50.0–500.0, and 20.0–200.0 ng mL^{-1} respectively. Average spike recoveries (mean ± standard deviation) are 93.3 ± 7.7%, 104.3 ± 6.6%, and 99.5 ± 9.0% respectively. The real concentrations in human plasma are 10.2 ± 0.3, 6.6 ± 0.1, and 5.3 ± 0.1 μg mL^{-1} respectively, which are consistent with the results obtained by LC–MS/MS method and reference values. In addition, we explored the third-order advantages through the real four-way array; it has shown that higher resolving power is one of the main advantages of higher-order tensor calibration method. These results demonstrated that the proposed method is sensitive, accurate, and efficient for direct quantitative analysis of aromatic amino acids in human plasma.

1. Introduction

L-phenylalanine, L-tyrosine, and L-tryptophan are α-amino acids and three of the building blocks of polypeptides and proteins. They participate in many functions of the living cell including, signal transduction, and transcription. As important small molecules, they also play important roles in metabolism, such as citric acid cycle. Phenylalanine, tyrosine, and tryptophan are formed from phosphoenolpyruvate and erythrose 4-phosphate, converted to a variety of important compounds in livings. Whether Phenylalanine, tyrosine, and tryptophan concentrations are too high or too low, the normal functions and metabolism of the body can be influenced. Given that the three aromatic amino acids are either neurotransmitters or precursors of neurotransmitters, genetic defects of aromatic amino acid metabolism can cause defective neural development and mental retardation [1]. For example, defective enzyme in phenylalanine metabolism results in excess phenylalanine, leading to the disease phenylketonuria (PKU). Therefore, quantitative analysis of phenylalanine, tyrosine, and tryptophan in biological fluid matrices is of biological significant.

The determination of these three analytes in such complex mixtures is feasible using enzyme sensor array [2] and analytical separations [3–5], such as gas or liquid chromatography–mass spectrometry (GC–MS or LC–MS), capillary electrophoresis–mass spectrometry (CE–MS). Chromatographic methods are highly selective and robust for these biologically relevant chemicals; however, analyte extraction and sample preparation are often required, which are time-consuming and laborious. In addition, the stage of analyte extraction may lose some amount of analyte, which makes bias in prediction of concentration level for analyte.

Considering that phenylalanine, tyrosine, and tryptophan have large bulky aromatic side chains with which the intrinsic fluorescence originates, fluorescence spectroscopy tends to be more attractive for quantitative analysis of them. Fluorescence spectroscopy can be applied to a wide range of problems in the chemical and biological sciences, and fluorescence detection is highly sensitive. However, fluorescence detection cannot provide high selectivity, especially for mixture. For quantitative analysis of phenylalanine, tyrosine, and tryptophan in human plasma, peculiar situations exist: using fluorescence signal at maximum emission wavelength, one can only determine one analyte at a time by

* Corresponding author. Tel./fax: +86 731 88821818.
E-mail address: hlwu@hnu.edu.cn (H.-L. Wu).

0039-9140/$ - see front matter © 2014 Elsevier B.V. All rights reserved.
http://dx.doi.org/10.1016/j.talanta.2014.01.036

purifying it from the other two analytes and plasma matrix, since the classical one-way (zero-order tensor) calibration method [6] requires signal must be fully selective for the analyte of interest. With the two-way (first-order tensor) multivariate calibration method [6–13], for example, based on fluorescence emission spectra, the three analytes can be determined simultaneously. However, the spectrum for the analyte of interest must be partially different from the spectra of all other responding species and, calibration standards must be representative of the samples containing any spectral interferent in human plasma [14]. As the rapid development of higher-order fluorescence instrument such as excitation–emission matrix fluorescence spectra (EEMs) [15], this prerequisite can be overcome through three-way (second-order tensor) calibration method [12,16–32]. This is due to the second-order advantage [6,33–35], which means analytes can be analyzed quantitatively even in the presence of uncalibrated interferents. One of most widely accepted models is the parallel factor analysis (PARAFAC) [36,37] (or called trilinear component model), ordinarily decomposed by alternating least-squares algorithm (PARAFAC-ALS) [20,35,38,39].

Because intrinsic protein fluorescence originates with the aromatic amino acids, the intrinsic protein fluorescence in human plasma overlaps seriously with that of phenylalanine, tyrosine, and tryptophan. This makes a challenge on the decomposition in three-way calibration method. Fortunately, the fluorescence intensity of each aromatic amino acid is strongly pH-dependent; this opens the possibility of introducing a pH mode to EEMs to construct four-way fluorescence excitation–emission–pH–sample (EEMs–pH) data array, on which four-way (third-order tensor) calibration method capable of providing higher resolving power [6,18,35,38,40–48] could be used.

As far as we know, simultaneous quantitative analysis of aromatic amino acids in human plasma by excitation–emission–pH intrinsic fluorescence coupled with four-way calibration has not been reported in previous works. This paper presents a novel fluorescence analytical method for simultaneous determination of phenylalanine, tyrosine, and tryptophan in human plasma with little preparation (Fig. 1). The method comprises four-way EEMs–pH measurements, data preprocessing of Rayleigh and Raman scattering using interpolation and four-way calibration. Preprocessing of the four-way array guarantees that the quadrilinear component model holds. Quadrilinear decomposition provides the pure excitation, emission, pH, and relative concentration profiles. Subsequently following the linear regression of decomposed relative concentration profile against real concentration for each analyte of interest which gives accurate prediction for calibration set, validation set, and real contents of analytes in human plasma respectively. Additionally, we explored the third-order advantages through the real four-way array.

2. Theory

2.1. Quadrilinear component model

In three-way (second-order tensor) calibration, one of the most commonly used models is the trilinear component model, which is often called as PARAFAC/CANDECOMP model, proposed by Harshman [36] and Caroll and Chang [37] independently. The concept of the trilinear component model can be naturally extended to the quadrilinear component model. Considering a model of the real-valued four-way array $\underline{\mathbf{X}}_{\boldsymbol{q}}$ with size of $I \times J \times K \times L$, in which each element x_{ijkl} can be expressed as follows:

$$x_{ijkl} = \sum_{n=1}^{N} a_{in} b_{jn} c_{kn} d_{ln} + e_{ijkl}$$
$$\text{for } i = 1,2,\ldots,I, \quad j = 1,2,\ldots,J, \quad k = 1,2,\ldots,K, \quad l = 1,2,\ldots,L. \tag{1}$$

where a_{in}, b_{jn}, c_{kn}, and d_{ln}, correspond to underlying profile matrices $\mathbf{A}_{I\times N}$, $\mathbf{B}_{J\times N}$, $\mathbf{C}_{K\times N}$, and $\mathbf{D}_{L\times N}$ of $\underline{\mathbf{X}}_{\boldsymbol{q}}$ respectively. The term e_{ijkl} is the element of the four-way residual array $\underline{\mathbf{E}}_{\boldsymbol{q}}$ with size of $I \times J \times K \times L$. Then the modeled part of x_{ijkl} is quadrilinear in the parameter sets a_{in}, b_{jn}, c_{kn}, and d_{ln}, In this work, $\mathbf{A}_{I\times N}$, $\mathbf{B}_{J\times N}$, $\mathbf{C}_{K\times N}$, and $\mathbf{D}_{L\times N}$, represent the excitation, emission, pH, and concentration profiles respectively, what successively make the first, second, third, and fourth mode of the four-way EEMs–pH data array.

Regardless of scaling and permutation, the decomposition of the quadrilinear component model will be a unique one [49,50] given that $k_{\mathbf{A}} + k_{\mathbf{B}} + k_{\mathbf{C}} + k_{\mathbf{D}} \geq 2F + 3$, where $k_{\mathbf{A}}, k_{\mathbf{B}}, k_{\mathbf{C}}$, and $k_{\mathbf{D}}$, are the k-ranks of the profile matrices $\mathbf{A}$, $\mathbf{B}$, $\mathbf{C}$, and $\mathbf{D}$, respectively.

In addition, the quadrilinear component model can be expressed as the following fully stretched matrix forms:

$$\mathbf{X}_{I\times JKL} = \mathbf{A}(\mathbf{D} \odot \mathbf{C} \odot \mathbf{B})^T + \mathbf{E}_{I\times JKL} \tag{2}$$

$$\mathbf{X}_{J\times KLI} = \mathbf{B}(\mathbf{A} \odot \mathbf{D} \odot \mathbf{C})^T + \mathbf{E}_{J\times KLI} \tag{3}$$

$$\mathbf{X}_{K\times LIJ} = \mathbf{C}(\mathbf{B} \odot \mathbf{A} \odot \mathbf{D})^T + \mathbf{E}_{K\times LIJ} \tag{4}$$

$$\mathbf{X}_{L\times IJK} = \mathbf{D}(\mathbf{C} \odot \mathbf{B} \odot \mathbf{A})^T + \mathbf{E}_{L\times IJK} \tag{5}$$

where $\odot$ indicates the Khatri-Rao product, Provided that matrices $\mathbf{A} \in \mathbb{R}^{I\times N}$ and $\mathbf{B} \in \mathbb{R}^{J\times N}$, their Khatri-Rao product is a matrix of size $(IJ) \times N$ and defined by

$$\mathbf{A} \odot \mathbf{B} = \begin{bmatrix} a_{11}\mathbf{b}_1 & a_{12}\mathbf{b}_2 & \cdots & a_{1N}\mathbf{b}_N \\ a_{21}\mathbf{b}_1 & a_{22}\mathbf{b}_2 & \cdots & a_{2N}\mathbf{b}_N \\ \vdots & \vdots & \ddots & \vdots \\ a_{I1}\mathbf{b}_1 & a_{I2}\mathbf{b}_2 & \cdots & a_{IN}\mathbf{b}_N \end{bmatrix}$$

2.2. Four-way PARAFAC method

In general, the four-way PARAFAC algorithm is carried out by alternating least-squares principle [38,39,41,43]. According to Eqs. (2)–(5), the updating presentations of four modes can be obtained as follows

$$\mathbf{A} = \mathbf{X}_{I\times JKL}((\mathbf{D} \odot \mathbf{C} \odot \mathbf{B})^T)^+ \tag{6}$$

$$\mathbf{B} = \mathbf{X}_{J\times KLI}((\mathbf{A} \odot \mathbf{D} \odot \mathbf{C})^T)^+ \tag{7}$$

$$\mathbf{C} = \mathbf{X}_{K\times LIJ}((\mathbf{B} \odot \mathbf{A} \odot \mathbf{D})^T)^+ \tag{8}$$

$$\mathbf{D} = \mathbf{X}_{L\times IJK}((\mathbf{C} \odot \mathbf{B} \odot \mathbf{A})^T)^+ \tag{9}$$

Through the decomposition of four-way array by the four-way PARAFAC algorithm, the relative profiles of the four different modes can be obtained. The decomposition of the quadrilinear component model joins the calibration set together with the prediction set, and then the concentration information can be obtained in a separate univariate regression step. In this work, we take the real concentration as the independent variable. The univariate regression is expressed as

$$\begin{bmatrix} y_1 \\ y_2 \\ \vdots \\ y_P \end{bmatrix} = \begin{bmatrix} 1 & x_1 \\ 1 & x_2 \\ \vdots & \vdots \\ 1 & x_P \end{bmatrix} \begin{bmatrix} b_0 \\ b_1 \end{bmatrix} + \begin{bmatrix} e_1 \\ e_2 \\ \vdots \\ e_P \end{bmatrix} \quad \text{In matrix notation is } \mathbf{y} = \mathbf{X}\mathbf{b} + \mathbf{e} \tag{10}$$

where P is the number of calibration samples. The model parameter is estimated by $(b_0, b_1)^{\mathrm{T}} = \mathbf{X}^+\mathbf{y}$. Then the analyte concentration is predicted by $\bar{x}_{\mathrm{unk}} = (y_{\mathrm{unk}} - \bar{b}_0)/\bar{b}_1$ for an unknown sample, where y_{unk} represents intensity in the decomposed relative concentration profile of the analyte.

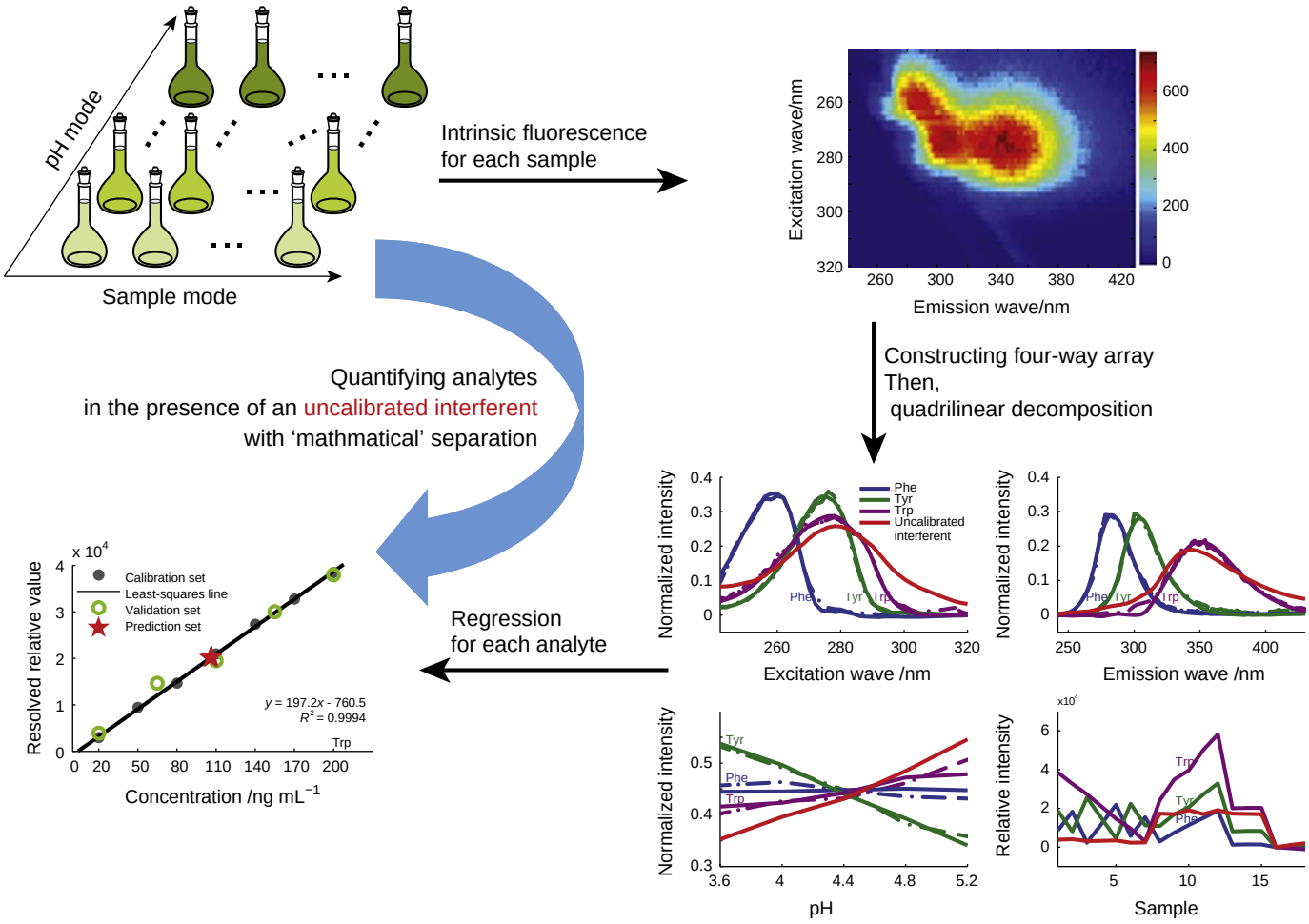

Fig. 1. Illustration of the multi-way intrinsic fluorescence calibration method.

In this study, we use random initialization to start the iterative optimizing procedure of four-way PARAFAC. The optimizing procedure is terminated when the following criterion is satisfied (in this study, we set the threshold $\varepsilon = 1 \times 10^{-9}$).

$$\left|\frac{\mathrm{SSR}^m - \mathrm{SSR}^{m-1}}{\mathrm{SSR}^{m-1}}\right| < \varepsilon \tag{11}$$

where SSR is residual sum of squares, $\mathrm{SSR}^m = \sum_{i=1}^{I}\sum_{j=1}^{J}\sum_{k=1}^{K}\sum_{l=1}^{L} e_{ijkl}^2$, and m is the current number of iterations. A maximal iteration number (10000) is adopted to avoid possible excess slow convergence.

2.3. Figures of merit

Figures of merit are analytical parameters used for evaluating performance of the calibration method. Different approaches have been discussed in the literature for computing figures of merit for higher-order methodologies.

The root mean square error of prediction (RMSEP) is computed [14] by

$$\mathrm{RMSEP} = \sqrt{\frac{1}{p}\sum_{p=1}^{P}(y_p - \bar{y}_p)^2} \tag{12}$$

where P is number of samples, y_p and $\bar{y}_p$ is the actual and predicted concentration respectively.

The sensitivity for analyte n can be computed by the following expression [51]:

$$\mathrm{SEN}_n = k_n / \|n\text{th row of}((\mathbf{I} - \mathbf{Z}_u\mathbf{Z}_u^{+})\mathbf{Z}_c)^{+}\| \tag{13}$$

where $\mathbf{Z}_c = [\mathbf{c}_{c1} \odot \mathbf{b}_{c1} \odot \mathbf{a}_{c1} \quad \cdots \quad \mathbf{c}_{cP} \odot \mathbf{b}_{cP} \odot \mathbf{a}_{cP}]$, associated to the P calibrated analytes, $\mathbf{Z}_u = [\mathbf{c}_{u1} \otimes \mathbf{b}_{u1} \otimes \mathbf{I}_a \quad \mathbf{c}_{u1} \otimes \mathbf{I}_b \otimes \mathbf{a}_{u1} \quad \mathbf{I}_c \otimes \mathbf{b}_{u1} \otimes \mathbf{a}_{u1} \quad \cdots \quad \mathbf{c}_{uQ} \otimes \mathbf{b}_{uQ} \otimes \mathbf{I}_a \quad \mathbf{c}_{uQ} \otimes \mathbf{I}_b \otimes \mathbf{a}_{uQ} \quad \mathbf{I}_c \otimes \mathbf{b}_{uQ} \otimes \mathbf{a}_{uQ}]$, containing information for the Q unexpected interferents.

The limit of detection (LOD) and limit of quantitation (LOQ) are estimated [52] as follows:

$$\mathrm{LOD} = 3.3 \times s(0) \tag{14}$$

$$\mathrm{LOQ} = 10 \times s(0) \tag{15}$$

where $s(0)$ is the standard error in the predicted concentration for method blank sample, computed by

$$s(0) = \sqrt{h_0 s_c^2 + h_0\frac{s_x^2}{\mathrm{SEN}^2} + \frac{s_x^2}{\mathrm{SEN}^2}} \tag{16}$$

where h_0 is the method blank sample leverage, s_c^2 is the variance in calibration concentrations, s_x^2 is the variance in the instrumental signal, and SEN is the analyte sensitivity.

3. Experimental

3.1. Apparatus and software

Fluorescence spectral measurements were performed on an F-7000 fluorescence spectrophotometer (HITACHI, Tokyo, Japan) equipped with a xenon lamp, and connected to a personal computer. All measurements were recorded in a 10 mm quartz cell at room temperature. The EEMs were recorded at emission wavelengths between 242 and 430 nm (every 2 nm), at different excitation wavelengths between 242 nm and 320 nm (every 2 nm). Excitation and emission slit widths were both set to be 5 nm, scan speed was set at 30,000 nm min^{-1}, and detector voltage was 600 V.

The LC–MS/MS analysis was performed on an Agilent 1290 series LC and a 6460 series triple quadrupole mass spectrometer (Agilent Technologies, Waldbronn, Germany) using an electrospray interface (ESI). ZORBAX Eclipse XDB-C18 (2.1 × 150 mm, 3.5 μm) analytical column (Agilent Technologies, Palo Alto, USA) was used for chromatographic separation. The mobile phase was 0.1% HAc aqueous: acetonitrile (93:07, v/v), which was pumped at a flow rate of 0.2 mL min^{-1} with 10 μL injection volume. The column temperature was 30 °C. MS/MS analysis was performed in positive ionization mode with the following conditions: drying gas flow 10 L/min, drying gas temperature 300 °C, nebulizer pressure 15 psi, sheath gas flow 7 L/min, sheat gas temperature 250 °C, nozzle voltage 1500 V and capillary voltage 4000 V. Nitrogen was used as the collision and nebulizing gas. Optimal settings for compound-dependent parameters are shown in Table S1.

The routines used were written in the MATLAB environment and run on a 3.07 GHz Intel (R) Core (TM) i7 CPU with 3 GB RAM under Windows 7 operating system.

3.2. Reagents and chemicals

L-phenylalanine (99%, Phe), L-tyrosine (99%, Tyr), and L-tryptophan (99%, Trp) were purchased from Aladdin (Aladdin, Shanghai, China). All other chemicals used were of analytical reagent grade, Acetonitrile (Oceanpak, Gothenburg, Sweden). Ultrapure water was produced by the Milli-Q Gradient A10 system (Millipore, Billerica, USA). The plasma was from YuanHengJinMa Biotechnology Development Co. (YuanHengJinMa, Beijing, China), Acetonitrile was added to human plasma in volume ratio of 2:1 for protein precipitation, the solution was vortexes for 20 s and then centrifuged for 10 min at 12,000 r/min [53].

Five buffer solutions were prepared by mixing appropriate amount of HAc and NaAc in ultrapure water, with pH 3.6, 4.0, 4.4, 4.8, and 5.2 respectively.

Individual stock solutions were prepared in 0.2 M HAc aqueous (Phe, Tyr, and Trp at a concentration of about 2000, 400, 200 μg mL^{-1} respectively). All the solutions were stored in the refrigerator at 4 °C.

3.3. Four-way data array

The calibration set consists of seven samples, designed by uniform design. For preparing a given calibration sample, the analytes were mixed in the volumetric flask, by taking appropriate volumes of Phe, Tyr, and Trp stock solutions and diluting to 10.00 mL with buffer of specific pH value. The validation set consists of five spiked samples. Each of them was prepared as follows: volume of 200.0 μL plasma was spiked with specific contents of all analytes (selected from their corresponding calibration ranges), and diluted to 10.00 mL with buffer of specific pH value. The prediction set consists of three plasma samples, which were used to determine the contents of Phe, Tyr, and Trp in real plasma sample. Three method blank samples also were prepared. In addition, three reference samples were prepared as reference. The details on the concentration designs are given in Table 1.

Table 1
The concentration designs of phenylalanine (Phe), tyrosine (Tyr), and tryptophan (Try).

Sample	Concentrations (ng mL^{-1})			Plasma (μL)
	Phe	Tyr	Try	
Calibration set				
cal01	8.0×10^3	350.0	200.0	
cal02	17.0×10^3	125.0	170.0	
cal03	2.0×10^3	500.0	140.0	
cal04	11.0×10^3	275.0	110.0	
cal05	20.0×10^3	50.0	80.0	
cal06	5.0×10^3	425.0	50.0	
cal07	14.0×10^3	200.0	20.0	
Validation set				
val01	2.0×10^3	50.0	20.0	200.0
val02	6.5×10^3	162.5	65.0	200.0
val03	11.0×10^3	275.0	110.0	200.0
val04	15.5×10^3	387.5	155.0	200.0
val05	20.0×10^3	500.0	200.0	200.0
Prediction set				
pre01				200.0
pre02				200.0
pre03				200.0

To introduce the pH mode, each of these samples was prepared five groups diluted by buffer of pH 3.6, 4.0, 4.4, 4.8, and 5.2, respectively. Then, fluorescence excitation-emission matrices as a function of pH were measured for each sample. Therefore, the measurement is a third-order tensor (excitation–emission–pH) per sample. With these third-order tensors for a group of samples, we can construct a four-way fluorescence excitation–emission–pH–sample data array (40 × 95 × 5 × 18).

4. Results and discussion

4.1. Preprocessing the EEMs–pH data array

In all samples severe Rayleigh and Raman scattering is present. These nonlinear factors can lead the four-way array to deviate the quadrilinear component model, which is a prerequisite for the four-way PARAFAC algorithm to decompose the profile of each mode correctly. Using the automated scatter identification method proposed by Bahram and Bro [54], we have handled scattering using interpolation in the areas affected by Rayleigh and Raman scattering (illustrated in Fig. S1).

Fig. 2 shows the preprocessed three-dimensional landscapes of fluorescence EEMs for calibration sample cal04 and prediction sample pre02 at pH 4.4. From the landscape of cal04, one can see that the spectra of Phe, Tyr, and Trp overlap seriously. For pre02, the maximum fluorescence intensity is about 1000, only one peak can be seen, although the plasma matrix is so complex that it may contains many fluorescence responsive constituents, there is no resolution among them. The spectra of spiked analytes totally overlap with that of plasma.

For quantitative analysis of the three aromatic amino acids based on fluorescence, one needs to extract the pure profiles of each analyte by physical–chemical separation or mathematical separation, then to predict the real concentrations of them, in the seriously overlapped peak among analytes and complex plasma matrix. The three-way calibration method might be the right one for mathematical separation. However, the overlap between

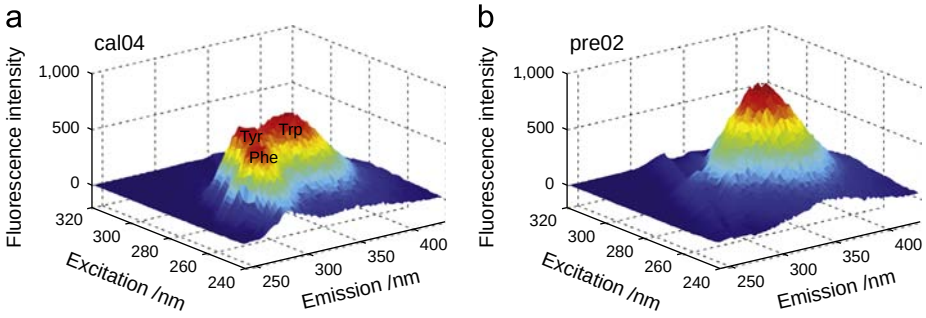

Fig. 2. Three-dimensional landscapes of fluorescence EEMs for sample cal04 and pre02 at pH 4.4.

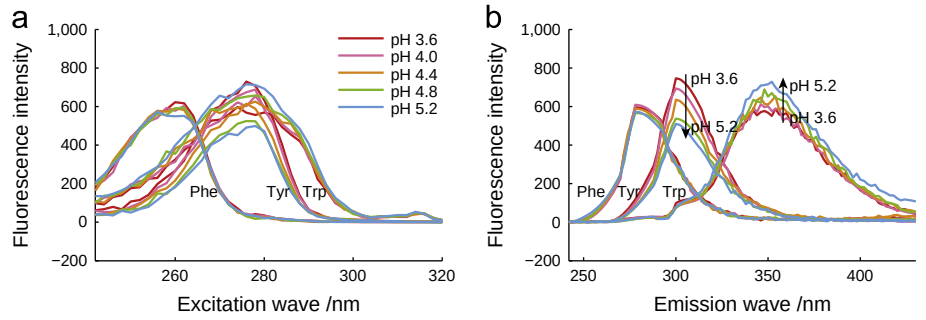

Fig. 3. The invariant on fluorescence spectra and the variation in fluorescence intensity of analytes with respect to different pH values.

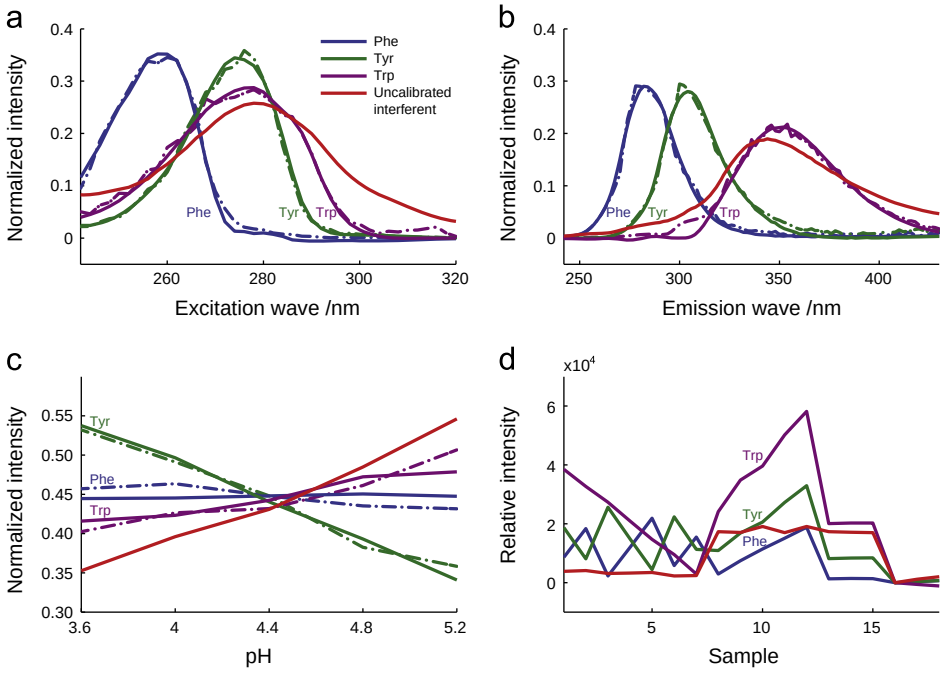

Fig. 4. Relative reference profiles (dash–dot lines) and decomposed profiles (solid lines) in each mode using the four-way PARAFAC ($N=4$).

spectra of Trp and that of plasma is too serious to extract the pure spectra of Trp; this may stem from the fact that the intrinsic fluorescence of remaining proteins is the primary unknown interferent in plasma and originates with the analytes of interest. The system studied is indeed a highly collinear and seriously interfering system. A valuable feature of intrinsic amino acids fluorescence is the high sensitivity to its local environment, such as pH value. Therefore, we introduced a pH mode to construct four-way data array, expect to solve this problem by four-way (third-order sensor) calibration method capable of providing higher resolving power.

4.2. Spectral properties of analytes at different pH

Because phenylalanine, tyrosine, and tryptophan are all acid–base amphoteric compounds, we carefully investigated their spectral properties at different pH values. Fig. 3 shows the excitation and emission spectra of each analyte are both invariant with respect to different pH values. This spectral property can guarantee that the quadrilinear component model will hold when introducing the pH mode.

As pH changes from 3.6 to 5.2, the fluorescence intensity of Tyr decreases, that of Phe slightly decreases, while the fluorescence

intensity of Trp increases. The pH profiles of analytes indicate that significance divergence can be introduced with the pH mode, which can strengthen the resolving power of four-way PARAFAC method. This might be an advantage of four-way calibration rather than three-way calibration.

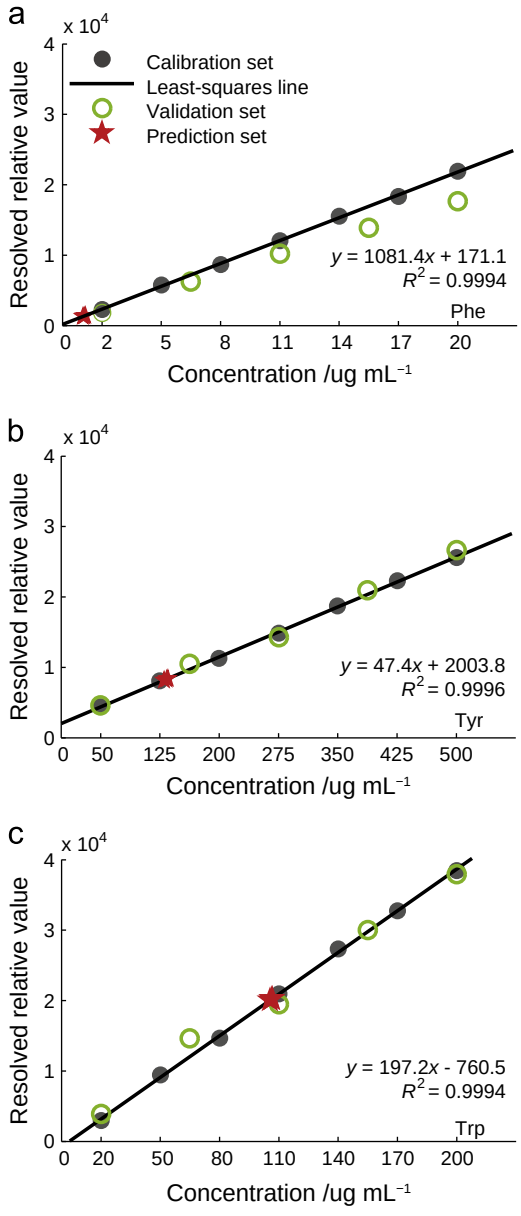

Fig. 5. Classical linear regression of decomposed relative concentration profile against concentrations for Phe, Tyr, and Trp respectively.

To explore the linear range of each analyte, a series of pure standards (at pH 4.4) were prepared for each analyte individually. For analytes Phe, Tyr, and Trp, the linear ranges are 1.0×10^3–40.0×10^3 (R^2=0.9992), 12.5–1375.0 (R^2=0.9996), and 5.0–550.0 (R^2=0.9997) ng mL^{-1} respectively. When designing the concentrations of calibration set, 10 times wide of range is used. In details, the selected linear calibration ranges of Phe, Tyr, and Trp are 2.0×10^3–20.0×10^3, 50.0–500.0, and 20.0–200.0 ng mL^{-1} respectively.

4.3. Estimation of the number of components

The number of components for the investigated system should be estimated before quadrilinear decomposition [36,37,55,56]. We used the method known as core consistency diagnostic to select the number of spectral components. It is given as the percentage of variation in a Tucker3 core array consistent with the theoretical superidentity array. When the core consistency drops from a high value (about 60%) to a low value, this indicates that an appropriate number of components have been attained. Considering the fact that rank determination is not always straightforward, especially in the presence of noise or complex matrix, also the chemical criteria (e.g. reference spectrum) and RMSEC are used to help in evaluating the appropriate number of components.

By joining the seven calibration samples, five validation samples, three prediction sample and three method blank samples together, a four-way data array of $40\times95\times5\times18$ is construct. For this four-way data array, the core consistencies are 100.00%, 46.3%, 27.3%, 0.1%, 0.0%, and 0.0% when N=1, 2, 3, 4, 5, and 6 respectively. With consideration of the reference spectrum and RMSEV, N=4 is a sensible choice for this four-way data array. Then we used the four-way PARAFAC algorithm with N=4 to decompose this quadrilinear component model, followed by classical linear regression for each analyte.

4.4. Testing the calibration model internally

One of the most important problems in the area of multivariate calibration is determining how effective a chemometric model is. Prior to the following analysis, we used the calibration set to testing the calibration model internally; the results of quantitative analysis for calibration set are listed in Table S2. For the calibration set, RMSECs of Phe, Tyr, and Trp are 0.1×10^3, 3.2, and 1.4 ng mL^{-1} respectively. Average recoveries (mean ± standard deviation) are 99.9 ± 2.2%, 100.3 ± 1.7%, and 99.5 ± 3.2% respectively. All these results distinctly indicate that the quadrilinear component model constructing on the EEMs–pH data is quite probably a good one.

Table 2
Predicted results for the validation set using the four-way calibration method.

Sample	Add concentrations (ng mL^{-1})			Predicted concentrations (ng mL^{-1}) [spike recovery %]		
	Phe	Tyr	Try	Phe	Tyr	Try
val01	2.0×10^3	50.0	20.0	[a]2.5×10^3 [127.0]	54.6 [109.3]	19.8 [99.1]
val02	6.5×10^3	162.5	65.0	6.7×10^3 [103.6]	180.3 [110.9]	74.2 [114.2]
val03	11.0×10^3	275.0	110.0	10.4×10^3 [94.6]	258.7 [94.1]	98.6 [89.7]
val04	15.5×10^3	387.5	155.0	13.8×10^3 [88.8]	400.6 [103.4]	152.2 [98.2]
val05	20.0×10^3	500.0	200.0	17.3×10^3 [86.3]	519.7 [103.9]	192.5 [96.3]
RMSEP (ng mL^{-1})				2.3×10^3	15.3	7.4
Average spike recovery ± standard deviation				93.3 ± 7.7%	104.3 ± 6.6%	99.5 ± 9.0%

[a] 127.0% is omitted as an outlier.

4.5. Prediction for validation set and prediction set

The validation set is used for method validation, to prove that the four-way calibration method can accurately predict the contents of Phe, Tyr, and Trp in the presence of uncalibrated interferents in plasma. Prediction set is used to determine the real contents of Phe, Tyr, and Trp in plasma.

Fig. 4 shows the relative reference profiles (dash–dot lines) and decomposed profiles (solid lines) in each mode using quadrilinear decomposition. From the decomposed profiles in each mode, one can see that this is indeed a high collinear and complex system. The decomposed excitation, emission, and pH profiles of each analyte are in good agreement with the reference profiles based on pure analyte standards. An uncalibrated spectral interferent

Table 3
Predicted results for the prediction set and figure of merits using the four-way calibration method.

Sample	Predicted concentrations (ng mL^{-1})		
	Phe	Tyr	Try
pre01	2.0×10^3	130.3	105.5
pre02	2.0×10^3	133.5	106.5
pre03	2.1×10^3	135.1	106.6
Mean ± standard deviation	$(2.0 \pm 0.1) \times 10^3$	133.0 ± 2.4	106.2 ± 0.6
Concentration levels in plasma (μg mL^{-1})	10.2 ± 0.3	6.6 ± 0.1	5.3 ± 0.1
Concentration levels by LC–MS/MS	9.8 ± 0.1	6.7 ± 0.1	5.0 ± 0.1
[a]$F_{calculated}$	9.0	1.0	1.0
[b]$t_{Calculated}$	1.8	1.0	3.0
Concentration levels in reference	7.8 ± 0.3	6.5 ± 0.9	6.3 ± 0.5
Figure of merits			
[c]SEN (mL ng^{-1})	0.9	20.4	14.3
LOD (ng mL^{-1})	191.9	23.9	3.0
LOQ (ng mL^{-1})	581.5	72.4	9.0

[a] $F_{calculated}$ is computed by $F = s_1^2/s_2^2$, where s_1 and s_2 are the standard deviations of the two methods. At the 95% confidence level, the critical value for F is 39.0.

[b] $t_{Calculated}$ is computed by $t = \bar{x}_1 - \bar{x}_2 / \sqrt{((n_1-1)s_1{}^2 + (n_2-1)s_2^2)/(n_1+n_2-2)}\sqrt{(1/n_1)+(1/n_2)}$, where $\bar{x}_1$ and $\bar{x}_2$ are the mean of the two methods respectively, n_1 and n_2 are the number of degrees of freedom of the two methods respectively. At the 95% confidence level, the critical value for t is 4.3.

[c] SEN is sensitivity.

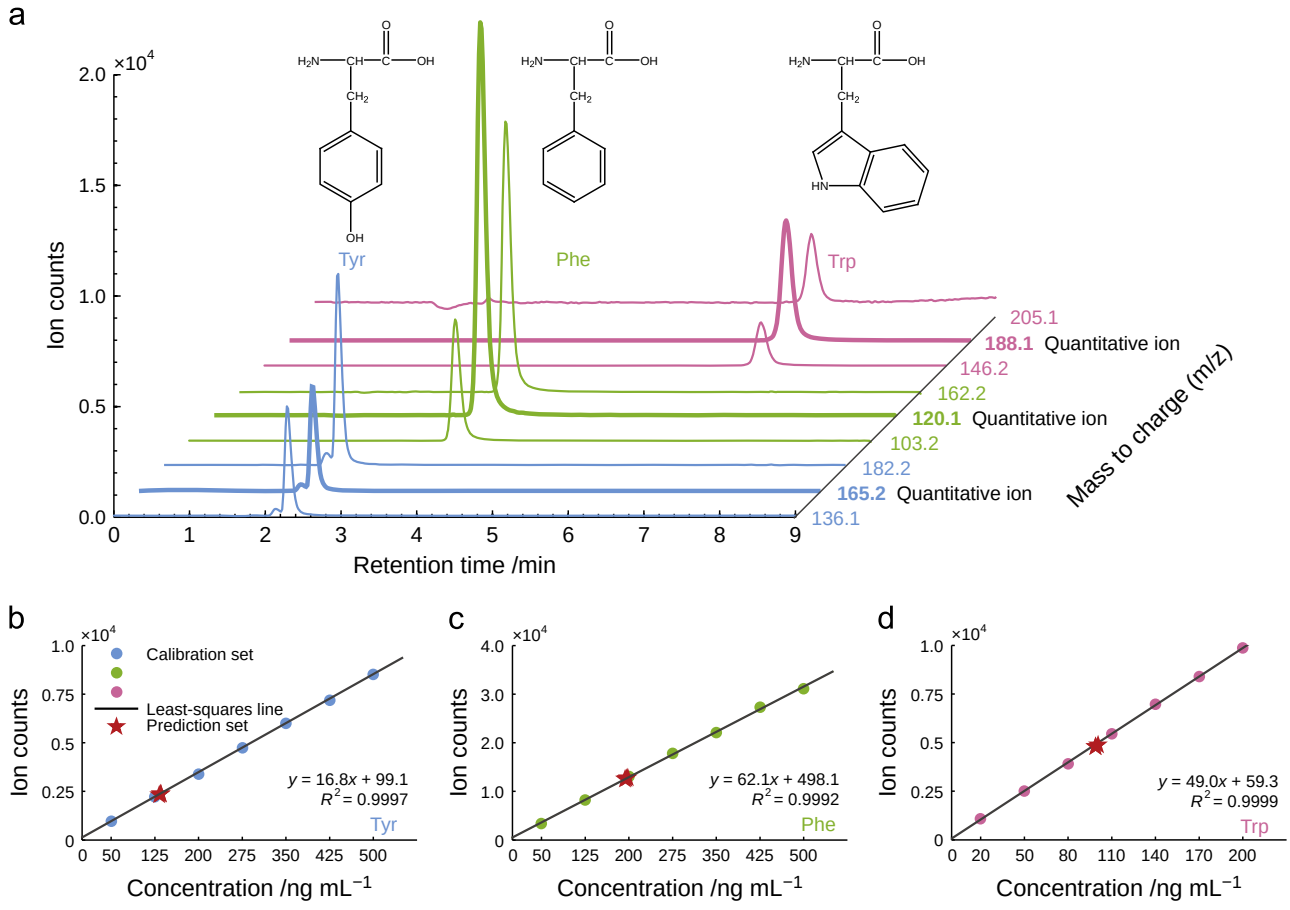

Fig. 6. Results of LC–MS/MS experiment. a: chromatographic separation; (b, c, and d) linear regression of Phe, Tyr, and Trp respectively.

was decomposed. Its profiles in every mode seriously overlap with that of analytes, especially in the fluorescence emission mode. In addition, we can see that the decomposed fluorescence spectra of analytes of interest is smoother than reference spectra, which indicates that four-way PARAFAC could smooth the decomposed profiles in decomposition process.

Fig. 5 shows the classical linear regression of decomposed relative concentration profile against real concentration for Phe, Tyr, and Trp respectively. The regression equations are $y=1081.4x+171.1$ ($R^2=0.9994$), $y=47.4x+2003.8$ ($R^2=0.9996$), and $y=197.2x-760.5$ ($R^2=0.9994$) for Phe, Tyr, and Trp respectively. The values of R^2 are all above 0.999, which deems a good linear fit for each analyte in the above-described range.

Spiking is one of the most common methods to evaluate accuracy. Therefore, the method validation was done by prediction for spike validation set; the results are given in Table 2. For Phe, Tyr, and Trp, RMSEPs are 2.3×10^3, 15.2, and 7.4 ng mL^{-1}and average spike recoveries (mean ± standard deviation) are 93.3 ± 7.7%, 104.3 ± 6.6%, and 99.5 ± 9.0% respectively. These results show that the accuracy of the proposed method is satisfying and reliable for the quantitative analysis of Phe, Tyr, and Trp in human plasma.

The prediction for prediction set is given in Table 3. It is worth noting that, for predicting the concentration level of Phe in human plasma, three additional prediction samples each containing 2.0 mL plasma in 10.0 mL were prepared (see Fig. S2), due to the poorer sensitivity of Phe compare to that of Tyr, and Trp. For the prediction samples, predicted concentrations (mean ± standard deviation) of Phe, Tyr, and Trp are $(2.0\pm0.1)\times10^3$, 133.0 ± 2.4, and 106.2 ± 0.6 ng mL^{-1}. In preparing each prediction sample, 2.0 mL plasma was diluted to 10.00 mL for Phe, 200.0 μL plasma was diluted to 10.00 mL for Tyr and Trp. Therefore, the real concentration levels of Phe, Tyr, and Trp in human plasma are 10.2 ± 0.3, 6.6 ± 0.1, and 5.3 ± 0.1 μg mL^{-1}. Table 3 also lists figures of merit. For Phe, Tyr, and Trp, SENs are 0.9, 20.4, 14.3 mL ng^{-1} respectively, LODs are 581.5, 72.4, and 9.0 ng mL^{-1} respectively.

In addition, the proposed method was compared with the approved LC–MS/MS method (see Fig. 6). The concentration levels of Phe, Tyr, and Trp in human plasma are identified as 9.8 ± 0.1, 6.7 ± 0.1, and 5.0 ± 0.1 μg mL^{-1}. Firstly, F test was performed [14]. As the each calculated value for F (9.0, 1.0, and 1.0 for Phe, Tyr, and Trp respectively) is lower than the critical value ($F_{\text{Table}}=39.0$), there is no significant difference in the variances from the two methods, at the 95% confidence level. Then, a two-tailed t test was applied [14]. Given that the each calculated value for t (1.8, 1.0, and 3.0 for Phe, Tyr, and Trp respectively) is lower than the critical value ($t_{\text{Table}}=4.3$), we accept the null hypothesis that there is no significant difference between the new method and the LC–MS/MS method. We could conclude that the two methods have similar precision and accuracy. Besides, the concentration levels of Phe, Tyr, and Trp in human plasma provided by the proposed method are consistent with that of reference [57].

All these results indicate that the proposed method can provide very sensitive and accurate prediction, with "mathematical separation" instead of "analytical separation", to determine Phe, Tyr, and Trp in the sophisticated matrix of human plasma simultaneously, in the presence of an unknown, uncalibrated spectral interferent.

5. Conclusion

Four-way calibration method based on the four-way PARAFAC algorithm has been applied for the simultaneous determination of L-phenylalanine, L-tyrosine, and L-tryptophan in human plasma, despite the uncalibrated serious interferent from the plasma. This is possible thanks to the third-order advantage, achieved when using four-way EEMs–pH array, because this approach allows for the quantitative analysis of analytes of interest in very complex matrices not only containing unknown, uncalibrated interferents but also existing high collinearity among spectra. The proposed analytical method has the advantages of being low cost, rapid, and environmentally friendly, with little sample preparation. The satisfying results obtained in this work indicate that the use of four-way EEMs–pH array in combination with four-way calibration method is a promising tool for multi-component simultaneous quantitative analysis in complex matrices.

Acknowledgments

The authors gratefully acknowledge the National Natural Science Foundation of China (Grant no. 21175041) and the National Basic Research Program (No. 2012CB910602) well as the Foundation for Innovative Research Groups of NSFC (Grant no. 21221003) for financial supports.

Appendix A. Supplementary material

Supplementary data associated with this article can be found in the online version at http://dx.doi.org/10.1016/j.talanta.2014.01.036.

References

[1] S.R. Bolsover, J.S. Hyams, E.A. Shephard, H.A. White, C.G. Wiedemann, Cell Biology: A Short Course, 2nd ed., John Wiley & Sons, New Jersey, USA, 2004.
[2] D.M. Bailey, A. Hennig, V.D. Uzunova, W.M. Nau, Chem,—Eur. J. 14 (2008) 6069–6077.
[3] J. Le Boucher, C. Charret, C. Coudray-Lucas, J. Giboudeau, L. Cynober, Clin. Chem. 43 (1997) 1421–1428.
[4] F.-Y. Tan, C. Tan, A.-P. Zhao, M.-L. Li, J. Agric. Food Chem. 59 (2011) 10839–10847.
[5] T. Soga, D.N. Heiger, Anal. Chem. 72 (2000) 1236–1241.
[6] A.C. Olivieri, Anal. Chem. 80 (2008) 5713–5720.
[7] H. Wold, E. Lyttkens, Bulletin of the International Statistical Institute: Proceedings of the 37th Session London, vol. 43 1969, pp. 29–51.
[8] Y.Z. Liang, O.M. Kvalheim, H.R. Keller, D.L. Massart, P. Kiechle, F. Erni, Anal. Chem. 64 (1992) 946–953.
[9] R. Tauler, B. Kowalski, S. Fleming, Anal. Chem. 65 (1993) 2040–2047.
[10] C. Demir, R.G. Brereton, Analyst 122 (1997) 631–638.
[11] X. Lin, Y. Ni, S. Li, S. Kokot, Analyst 137 (2012) 2086–2094.
[12] Y. Wang, X. Ma, Y. Wen, J. Liu, W. Cai, X. Shao, Anal. Methods 4 (2012) 2893–2899.
[13] S.P. Schale, T.M. Le, K.M. Pierce, Talanta 94 (2012) 320–327.
[14] P. Gemperline, Practical Guide to Chemometrics, 2nd ed., CRC press, Boca Raton, FL, USA, 2006.
[15] K.S. Booksh, A.R. Muroski, M. Myrick, Anal. Chem. 68 (1996) 3539–3544.
[16] E. Sanchez, B.R. Kowalski, Anal. Chem. 58 (1986) 496–499.
[17] B.E. Wilson, W. Lindberg, B.R. Kowalski, J. Am. Chem. Soc. 111 (1989) 3797–3804.
[18] P. Geladi, Chemom. Intell. Lab. Syst. 7 (1989) 11–30.
[19] E. Sanchez, B.R. Kowalski, J. Chemom. 4 (1990) 29–45.
[20] H.-L. Wu, M. Shibukawa, K. Oguma, J. Chemom. 12 (1998) 1–26.
[21] Z.-P. Chen, H.-L. Wu, J.-H. Jiang, Y. Li, R.-Q. Yu, Chemom. Intell. Lab. Syst. 52 (2000) 75–86.
[22] Y. Tan, J.-H. Jiang, H.-L. Wu, H. Cui, R.-Q. Yu, Anal. Chim. Acta 412 (2000) 195–202.
[23] J.A. Arancibia, A.C. Olivieri, D.B. Gil, A.E. Mansilla, I. Durán-Merás, A.M. de la Peña, Chemom. Intell. Lab. Syst. 80 (2006) 77–86.
[24] R. Tauler, Chemom. Intell. Lab. Syst. 30 (1995) 133–146.
[25] T.G. Kolda, B.W. Bader, SIAM Rev. 51 (2009) 455–500.
[26] A.M. de la Peña, A.E. Mansilla, D.G. Gómez, A.C. Olivieri, H.C. Goicoechea, Anal. Chem. 75 (2003) 2640–2646.
[27] J. Liu, X. Ma, Y. Wen, Y. Wang, W. Cai, X. Shao, Ind. Eng. Chem. Res. 50 (2011) 7677–7681.
[28] H. Chen, J.E. Kenny, Analyst 137 (2012) 153–162.
[29] A. Gredilla, J. Amigo, S.F.-O. de Vallejuelo, A. de Diego, R. Bro, J. Madariaga, Anal. Methods 4 (2012) 676–684.
[30] S. Mas, A. de Juan, R. Tauler, A.C. Olivieri, G.M. Escandar, Talanta 80 (2010) 1052–1067.
[31] Y. Zhang, H.-L. Wu, A.L. Xia, Q.-J. Han, H. Cui, R.-Q. Yu, Talanta 72 (2007) 926–931.
[32] J.-Y. Wang, H.-L. Wu, Y. Chen, M. Zhai, X.-D. Qing, R.-Q. Yu, Talanta 116 (2013) 347–353.

[33] K.S. Booksh, B.R. Kowalski, Anal. Chem. 66 (1994) 782–791.
[34] G.M. Escandar, A.C. Olivieri, N.K.M. Faber, H.C. Goicoechea, A. Muñoz de la Peña, R.J. Poppi, TrAC Trends Anal. Chem. 26 (2007) 752–765.
[35] A.K. Smilde, Chemom. Intell. Lab. Syst. 15 (1992) 143–157.
[36] R.A. Harshman, UCLA Working Papers in Phonetics, vol. 16, 1970. pp. 1–84.
[37] J.D. Carroll, J.-J. Chang, Psychometrika 35 (1970) 283–319.
[38] P. Paatero, J. Comput. Graph Stat. 8 (1999) 854–888.
[39] R. Bro, Chemom. Intell. Lab. Syst. 38 (1997) 149–171.
[40] A.C. Olivieri, J.A. Arancibia, A.M. de la Peña, I. Duran-Meras, A.E. Mansilla, Anal. Chem. 76 (2004) 5657–5666.
[41] M.L. Nahorniak, G.A. Cooper, Y.-C. Kim, K.S. Booksh, Analyst 130 (2005) 85–93.
[42] M.A. de la Peña, I. Durán Merás, A. Jiménez Girón, Anal. Bioanal. Chem. 385 (2006) 1289–1297.
[43] A.-L. Xia, H.-L. Wu, S.-F. Li, S.-H. Zhu, L.-Q. Hu, R.-Q. Yu, J. Chemom. 21 (2007) 133–144.
[44] A.C. Olivieri, J. Chemom. 19 (2005) 253–265.
[45] H.-L. Wu, J.-F. Nie, Y.-J. Yu, R.-Q. Yu, Anal. Chim. Acta 650 (2009) 131–142.
[46] S.-F. Li, H.-L. Wu, L. Huang, Y.-N. Li, J.-F. Nie, S.-R. Zhang, R.-Q. Yu, Anal. Methods 2 (2010) 1069–1077.
[47] A.C. Olivieri, Anal. Methods 4 (2012) 1876–1886.
[48] C. Kang, H.-L. Wu, Y.-J. Yu, Y.-J. Liu, S.-R. Zhang, X.-H. Zhang, R.-Q. Yu, Anal. Chim. Acta 758 (2013) 45–57.
[49] J.B. Kruskal, Linear Algebra Appl. 18 (1977) 95–138.
[50] N.D. Sidiropoulos, R. Bro, J. Chemom. 14 (2000) 229–239.
[51] A.C. Olivieri, K. Faber, Anal. Chem. 84 (2012) 186–193.
[52] A.C. Olivieri, N.K.M. Faber, Chemom. Intell. Lab. Syst. 70 (2004) 75–82.
[53] C. Polson, P. Sarkar, B. Incledon, V. Raguvaran, R. Grant, J. Chromatogr. B 785 (2003) 263–275.
[54] M. Bahram, R. Bro, C. Stedmon, A. Afkhami, J. Chemom. 20 (2006) 99–105.
[55] P.J. Gemperline, J. Chem. Inf. Comp. Sci. 24 (1984) 206–212.
[56] R. Bro, H.A. Kiers, J. Chemom. 17 (2003) 274–286.
[57] R.J. Wurtman, C.M. Rose, C. Chou, F.F. Larin, New Engl. J. Med. 279 (1968) 171–175.